

Inductive Plasma Thruster (IPT) Design for an Atmosphere-Breathing Electric Propulsion System (ABEP)

F. Romano^{a,1}, Y.-A. Chan^{a,2}, G. Herdrich^{a,3}, C. Traub^a, S. Fasoulas^a,
P.C.E. Roberts^b, K. Smith^b, S. Edmondson^b, S. Haigh^b, N.H. Crisp^b,
V.T. A. Oiko^b, S.D. Worrall^b, S. Livadiotti^b, C. Huyton^b, L.A. Sinpetru^b,
A. Straker^b, J. Becedas^c, R.M. Domínguez^c, D. González^c, V. Cañas^c,
V. Sullioti-Linner^c, V. Hanessian^d, A. Mølgaard^d, J. Nielsen^d, M. Bisgaard^d,
D. Garcia-Almiñana^e, S. Rodriguez-Donaire^e, M. Sureda^e, D. Kataria^f,
R. Outlaw^g, R. Villain^h, J.S. Perez^h, A. Conte^h, B. Belkouchi^h, A. Schwalberⁱ,
B. Heißererⁱ

^a*Institute of Space Systems (IRS), University of Stuttgart, Stuttgart, 70569, Germany*

^b*The University of Manchester, George Begg Building, Sackville Street, Manchester, M13 9PL, UK*

^c*Elecnor Deimos Satellite Systems, C/ Francia 9, 13500, Puertollano, Spain*

^d*GomSpace AS, Langagervej 6, Aalborg East 9220, Denmark*

^e*UPC-BarcelonaTECH, Colom 11, TR5 - 08222 Terrassa, Spain*

^f*Mullard Space Science Laboratory, University College London Holmbury St. Mary, Dorking, Surrey, RH5 6NT, UK*

^g*Christopher Newport University, Newport News, Virginia 23606, United States*

^h*Euroconsult, 86 Boulevard de Sébastopol, Paris, France*

ⁱ*concentris research management gmbh, Ludwigstraße 4, Fürstenfeldbruck, 82256, Germany*

Abstract

Challenging space missions include those at very low altitudes, where the atmosphere is source of aerodynamic drag on the spacecraft, therefore an efficient propulsion system is required to extend the mission lifetime. One solution is Atmosphere-Breathing Electric Propulsion (ABEP). It collects atmospheric particles to be used as propellant for an electric thruster. This would minimize the requirement of limited propellant availability. The system could be applied to any planet with atmosphere, enabling new mission at low altitude ranges for longer times. Challenging is also the presence of reactive chemical species, such as atomic oxygen in Earth orbit. Such components are erosion sources of (not only) propulsion system components, i.e. acceleration grids, electrodes, and discharge channels of conventional EP systems (RIT and HET). IRS is developing, within the DISCOVERER project, an intake and a thruster for an ABEP system. This paper deals with the design and implementation of the inductive

¹Research Associate, romano@irs.uni-stuttgart.de

²Research Associate, chan@irs.uni-stuttgart.de

³Head Plasma Wind Tunnels and Electric Propulsion, herdrich@irs.uni-stuttgart.de

plasma thruster (IPT) developed at IRS. The paper describes its design aided by numerical tools such as HELIC and ADAMANT for the plasma, and XFDTD for the antenna design. Such a device is based on RF electrodeless discharge aided by externally applied DC magnetic field. The IPT is composed by a movable injector, to variate the discharge channel length, and a movable electromagnet to variate position and intensity of the magnetic field. By changing these parameters along with a novel antenna design for electric propulsion based on the birdcage, the aim is to achieve the highest efficiency for the RF circuit, and for the ionization stage. This is also aimed to be aided by the formation of helicon wave-based discharge. Finally, the designed IPT is presented and the feature of the birdcage antenna highlighted.

Keywords: ABEP - IPT - VLEO - Helicon - Birdcage

Nomenclature

ABEP: Atmosphere-Breathing Electric Propulsion

IPT: Inductive Plasma Thruster

VLEO: Very Low Earth Orbit

S/C: Spacecraft

1. Introduction

The Inductive Plasma Thruster (IPT) is designed at IRS within the EU H2020 DISCOVERER project that aims to redesign very low Earth orbit (VLEO $h < 400$ km) platforms by researching on low drag materials, aerodynamic attitude control systems, and by the development of an Atmosphere-Breathing Electric Propulsion system (ABEP) [1–7]. Orbiting in VLEO can open a new range of space missions [8], however, the mission lifetime is limited due to aerodynamic drag. To enable longer missions, the spacecraft requires a propulsion system that compensates the drag in an efficient matter. An ABEP system is hereby proposed as a solution. In an Atmosphere-Breathing Electric Propulsion (ABEP) system, an intake collects the residual atmosphere of a celestial body, and use it to feed an electric thruster. This ionizes and accelerates the atmospheric particles to produce thrust, see Fig. 1. An ABEP system theoretically removes the lifetime limits due to drag and due to the limited availability of propellant aboard the spacecraft. The propulsion system, in Earth orbit, must operate with N_2 and atomic oxygen O as propellants [3]. An ABEP system is not only applicable for Earth orbiting spacecrafts, but also to any celestial body with atmosphere given that enough electric power is provided. Within DISCOVERER, an RF-based contact-less thruster, the IPT, is developed. With such characteristic, any issue given by the use of reactive propellants, such as atomic oxygen, that can erode thruster components is removed. The IPT, moreover, is a neutralizer free device, as the exhaust plume is already neutral.

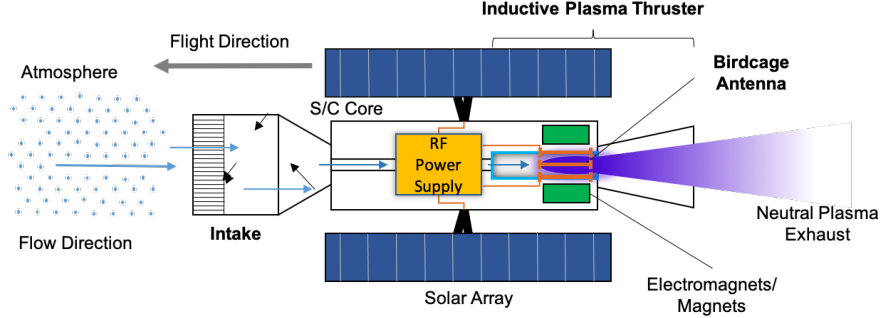


Figure 1: Atmosphere-Breathing Electric Propulsion Concept using an IPT.

2. Inductive Plasma Thruster Design

The starting point of the IPT development has been the heritage of IRS on inductive plasma generators (IPG) [9–11]. Major upgrades have been performed for the small-scale IPG6-S in the last years, such device is based on a coil-type antenna fed at 4 MHz up to 3.5 kW input power, but not designed for propulsion purposes, [3, 4, 12]. Recent test campaigns have shown a large increase of power absorption by applying an external magnetic field to IPG6-S [13], and hence confirmed the feasibility of an improved plasma source that makes use of applied static magnetic fields, especially as it can possibly trigger helicon wave-modes [14]. The requirements within DISCOVERER are of an RF contact-less plasma thruster operated with variable mixtures of N_2 and O as propellant with $P_{in} < 5$ kW. To cope with the chemically aggressive atomic oxygen, one of the main species in VLEO, IPT is designed to minimize any direct contact with the plasma, so to reduce erosion issues. In conventional EP systems, such as gridded ion thrusters and Hall-effect thruster, the operation with atomic oxygen causes erosion of grids and discharge channels, and will rapidly reduce thruster’s performance over time [15], [16]. The IPT, is designed to generate a neutral plasma plume that does not require a neutralizer, a device that requires a challenging, especially when fed with Earth’s atmospheric mixtures [17], [18]. The first version of the IPT is a laboratory model designed for maximum (technical) flexibility and passive cooling, to allow easy modifications for optimization purposes. Following the design of mechanical and vacuum interfaces [19], the crucial element of the IPT design is the antenna which will be described in the following sections.

3. Antenna Design

The antenna of the IPT, is the RF-fed component that creates the electromagnetic (EM) fields required for the ionization (mainly) and acceleration of the injected propellant. According to results from HELIC and ADAMANT [13] numerical tools, a frequency higher than 27.12 MHz is preferable, as this leads

to easier ignition and better power absorption at higher plasma densities when associated with an externally applied DC magnetic field [4, 20, 21]. Finally, an RF-Generator and an auto-matching network operating at 40.68 MHz for a power up to 4 kW have been acquired at IRS. The first antenna design approach has been that of a coil-type. Simulations show that coil-type antennas perform better than half-helical antennas, that more commonly used in helicon plasma sources [13]. The discharge channel has been selected with 37 mm inner diameter (same as IPG6-S), by setting a variable number of turns coil-type antenna. Many coil-type antennas configuration, with different number of turns and pitches have been evaluated by using both HELIC [22], [23], and ADAMANT [24] tools. An RF-based plasma source can be modelled as a transformer, where the plasma is seen as the secondary winding of the circuit and modelled as an impedance in the circuit. According to Chen [14], the plasma resistance R_P must be high, at least higher than the circuit resistance R_C so to maximize power absorption at the antenna, rather than in the circuitry. Finally, antenna and plasma have to be rather modelled as an equivalent impedance Z , with both real (resistance R) and imaginary (reactance X) components. In particular, the reactance X , is partly directly proportional to the applied frequency and has to be zeroed, to minimize power reflection. A power supply operating at $f = 40.68$ MHz introduces an “a priori” higher reactance due to its frequency, especially by implementing a coil-type antenna. Such reactance is a mismatch and power loss source in the RF circuit that needs to be compensated. ADAMANT, compared to HELIC, gives as output the impedance Z , of the antenna plus the plasma in both R and X , see Eq. 1.

$$\begin{aligned}\vec{Z} &= \vec{R} + j\vec{X} \\ X &= X_L + X_C = 2\pi fL + \left(\frac{1}{2\pi fC}\right)\end{aligned}\tag{1}$$

The numerical results for various plasma densities, magnetic fields, and coil antennas configurations, always resulted in a very high reactance X . Moreover, not only the antenna is to be considered for the thruster design, but the system at the whole, including the RF generator, its matching network, connectors, and cables [25]. In an RF circuit, the power transfer from a source (RF generator) to its load (antenna and plasma) is maximized only if the load’s impedance Z_L is matched to that of the source Z_S . RF generators standards is $Z_S = 50 + j0\Omega$ purely resistive output. The matching network is introduced to create a resonant circuit with the load that is dynamically matched to Z_S by a system of variable inductors and capacitors. This works mainly as protection for the RF generator, but it does not improve the load itself. Therefore, an optimum design of the antenna is required to maximize the power transfer from source to load. Plasma is finally a variable impedance that implies the need of a dynamic tuning control. An accurate selection of cabling, connectors and finally the antenna has been performed. The schematics describing the simplified RF circuit of the IPT including respective RF generator, matching network and connecting cables, is shown in Fig. 2.

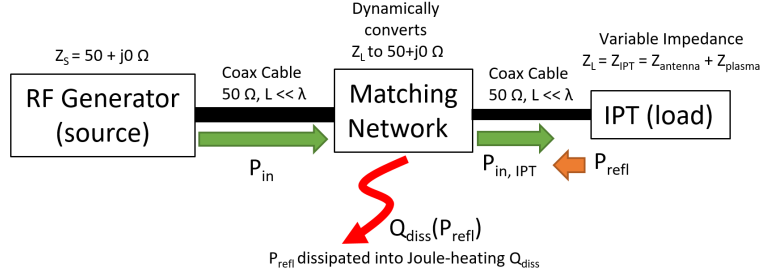


Figure 2: Simplified IPT RF circuit [6].

4. The Birdcage Antenna

The seek of RF circuit optimization lead to the birdcage antenna. Such device has been developed in Magnetic Resonance Imaging (MRI) [26] and provides the very homogeneous magnetic field required by the application. Birdcage antennas operate on the principle that a sinusoidal current distribution over a cylindrical surface will induce a homogeneous transversal magnetic field within the cylindrical volume itself. Such antennas are made by two end-rings, connected by equally spaced legs. The legs and/or the end-rings have capacitors in between to adjust the resonance frequency to the one required. Birdcage antennas can be designed as low-pass, high-pass, or band-pass frequency response depending on capacitor locations, see Fig. 3.

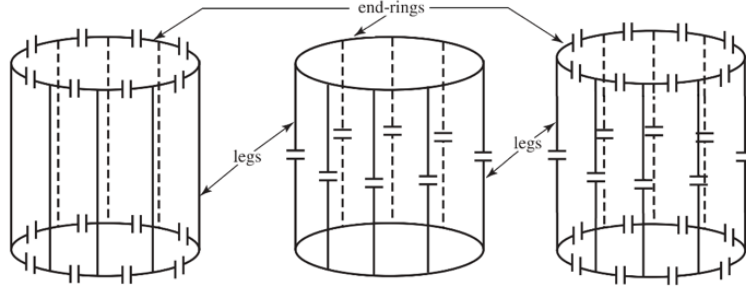


Figure 3: Birdcage Antenna: high-pass (left), low-pass (middle), band-pass (right), adapted from [27].

By operating birdcage antennas at one of their resonance frequencies, X is zero and its impedance Z is purely real. In such way, the load is already partially matched and only the resistance R requires further matching. Moreover, at a certain resonance frequency mode, the electromagnetic (EM) fields are perpendicular to each other and homogeneous within the cross section of the enclosed cylindrical volume. Depending on the feeding such fields are linearly or circularly polarized. Concerning plasma application, EPFL and Helyssen Sarl are the only known entity generating helicon plasma for fusion research by birdcage

antennas operating at 13.56 MHz at up to 10 kW [28–30]. Moreover, an older study from Guittienne directly investigated the use of birdcage antennas for an helicon based thruster [31]. Each birdcage antenna has generally $k = N/2$ resonance modes. The current distribution along the antenna follows the law described in Eq. 2, where I_{jk} is the normalized current at the j -th loop for the k -th mode of a birdcage antenna with N legs.

$$I_{jk} = \begin{cases} \cos(\frac{2\pi jk}{N}); & k = 0, 1, 2, \dots, N/2 \\ \sin(\frac{2\pi jk}{N}); & k = 1, 2, \dots, (N/2 - 1) \end{cases} \quad (2)$$

Therefore, the more legs are implemented, the better the current distribution matches a sinusoidal curve, see Fig. 4. On a single leg, instead, the amplitude of current variates over time as shown in Fig. 5. Birdcage antennas are modelled

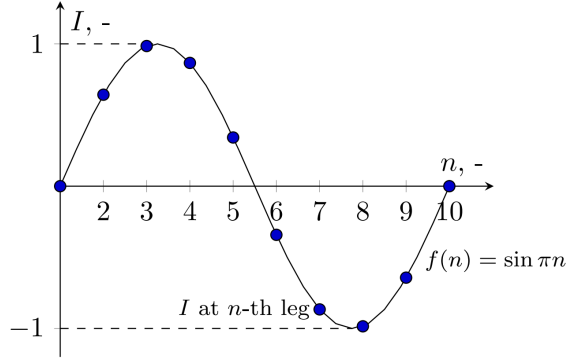


Figure 4: Birdcage Antenna current distribution along a 10-leg birdcage at a given time.

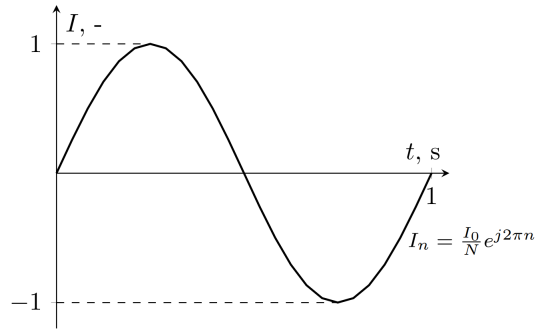


Figure 5: Birdcage Antenna current amplitude over time on a single leg.

by self and mutual inductances of legs and end-rings (ER) L_{Leg} and L_{ER} , plus the applied capacitors of capacitance C . Resonance frequencies for the high pass design are given in Eq. 3. The high pass design has one resonance mode

more ($k = 0$) at the highest frequency called anti-resonant AR.

$$\omega_{k_{HP}} = \left[C \left(L_{ER} + 2L_{Leg} \sin^2 \frac{\pi k}{N} \right) \right]^{-1/2}, \quad (k = 0, 1, 2, \dots, N/2) \quad (3)$$

Only one resonant mode at $k = 1$ presents the desired EM fields configuration. In terms of EM fields, the magnetic field created by the birdcage is \vec{B}_1 along y , the respective electric field \vec{E}_1 is perpendicular to \vec{B}_1 , along x , see Fig. 6. Since \vec{B}_1 is linearly polarized, its direction will switch along y on each cycle, and, therefore, so will \vec{E}_1 along x . An additional external DC magnetic field is provided along the z axis \vec{B}_0 to aid the formation of helicon waves.

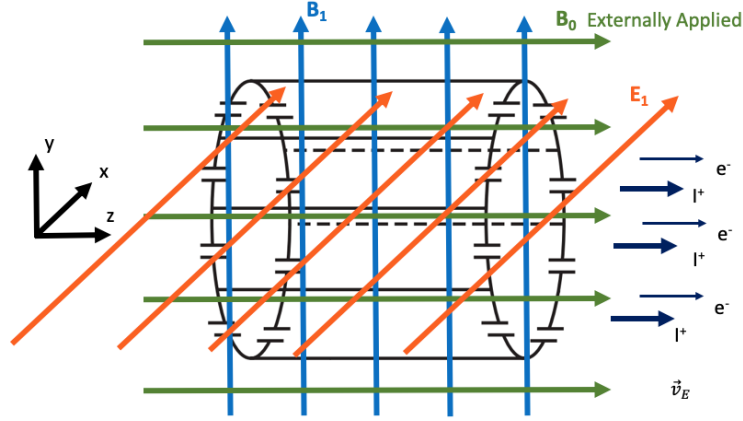


Figure 6: Birdcage EM fields \vec{B}_1, \vec{E}_1 , externally applied magnetic field \vec{B}_0 .

The resulting EM fields, which still exclude those of the plasma, provide a drift (exhaust) velocity $\vec{v}_E = \vec{E} \times \vec{B}$. This is imparted to both ions and electrons along the same direction on z . Correspondingly, thrust and exhaust velocity of significance are already provided by this mode while also ensuring a quasi-neutral plasma exhaust that will not require the implementation of a neutralizer, see Eq. 4. Such results support the use of a birdcage antenna for a contact-less plasma thruster application without needing a neutralizer. The y -component of the drift, instead, is zeroed at each cycle.

$$\vec{v}_E = \frac{1}{B^2} \begin{vmatrix} \hat{x} & \hat{y} & \hat{z} \\ E_1 & 0 & 0 \\ 0 & B_1 & B_0 \end{vmatrix} = \frac{1}{B_0^2 + B_1^2} \begin{Bmatrix} 0 \\ -E_1 B_0 \\ E_1 B_1 \end{Bmatrix} \quad (4)$$

5. IPT Design with a Birdcage Antenna

The IPT is made of the following main components: the propellant injector, the discharge channel, the birdcage antenna, the shield, the electromagnet and the support structure, see Fig. 7. The injector is movable along the symmetry

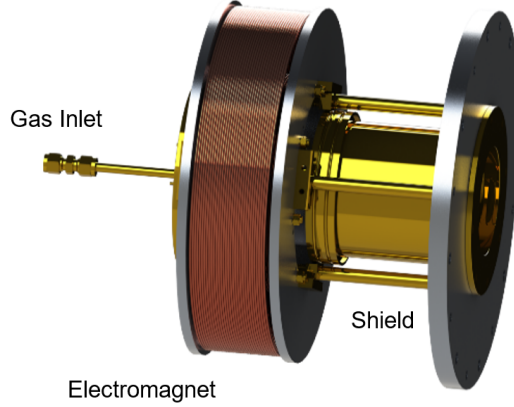


Figure 7: IPT rendering with external electromagnet.

axis z , as well as the external electromagnet, that can produce a magnetic field up to 70mT with 15 A DC current. At such current, more than 30 min operation are possible without overheating. This to allow plasma diagnostic measurements to be performed. A birdcage with 8 legs in a high pass design has been chosen and designed for resonance at 40.68 MHz in the $k = 1$ mode, feeding is provided at one point that leads to a linear polarization of the EM fields. Commercial 3D EM simulation software Remcom Inc. XFDTD® 7.8.1.3 is used to evaluate the resonance spectrum, the corresponding impedances, the EM fields, and the resulting required capacitance. The IPT structure is made of brass to minimize Eddy currents due to the RF fields, and to minimize interactions with the externally applied DC magnetic field. Enclosed within a brass RF shield is the birdcage antenna. It isolates the outer environment from the EM fields created by the birdcage and vice versa. Mechanical design is such to allow mounting on standard ISO-K flanges therefore minimizing the in-house required parts and enabling testing on standard facilities. In XFDTD, frequency is swept as signal input to the antenna, and the resulting impedance Z and scattering parameter S_{11} over frequency are plotted. The S_{11} parameter is generally defined as the input port voltage reflection coefficient. It represents how much power is absorbed and reflected by a load depending on the input at the signal source. The resonance study is shown within S_{11} and for Z in Fig. 8 and Fig. 9 from XFDTD. Correspondingly estimated required capacitance to match the desired resonance frequency mode is of $C = 785.51$ pF. Each peak of S_{11} is a resonance frequency, correspondingly the reactance goes to 0 at that same frequency. Indeed, there are $N/2 = 4$ resonance modes plus the AR one at the highest frequency. To verify that the $k = 1$ is the correct one, the 3D EM fields are extracted and visualized, see Fig. 10, over time in the cylindrical cross section enclosed by the birdcage. Those are compared to that of each of the other peaks. An example of the correct resonance with a linearly polarized field is shown in Fig. 10 (top) for the magnetic field and in Fig. 10 (bottom)

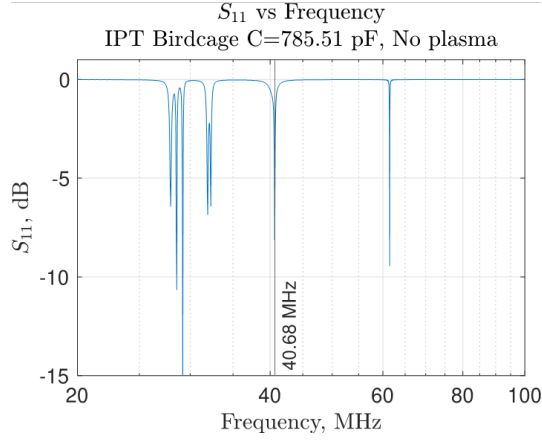


Figure 8: S_{11} vs Frequency IPT.

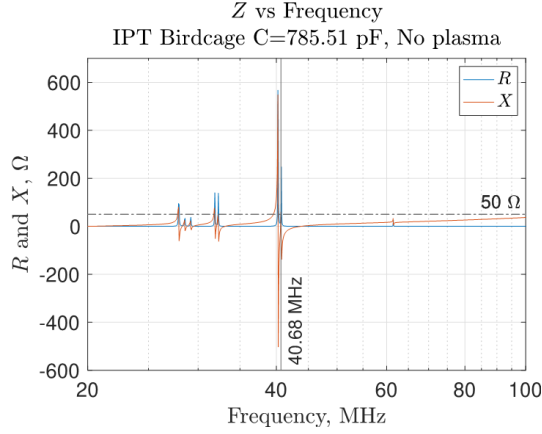


Figure 9: Z vs Frequency IPT.

for the electric field [6]. At each RF cycle the EM fields reverse their direction. Once the correct resonance peak is identified, the capacitance is swept until the peak is at 40.68 MHz. The externally applied magnetic field is expected to aid the formation of helicon waves within the discharge channel therefore providing a high degree of ionization [14], [32]. As can be seen, the resonance frequency presents a relatively low S_{11} parameter that translates in the fact that the real part R of the impedance Z is not matched to that of the RF generator output, and that requires further matching/tuning of R only.

6. Resonance Tuning

The design for resonance ensures that such condition is maintained without plasma. Once the plasma is ignited, a frequency shift and a corresponding

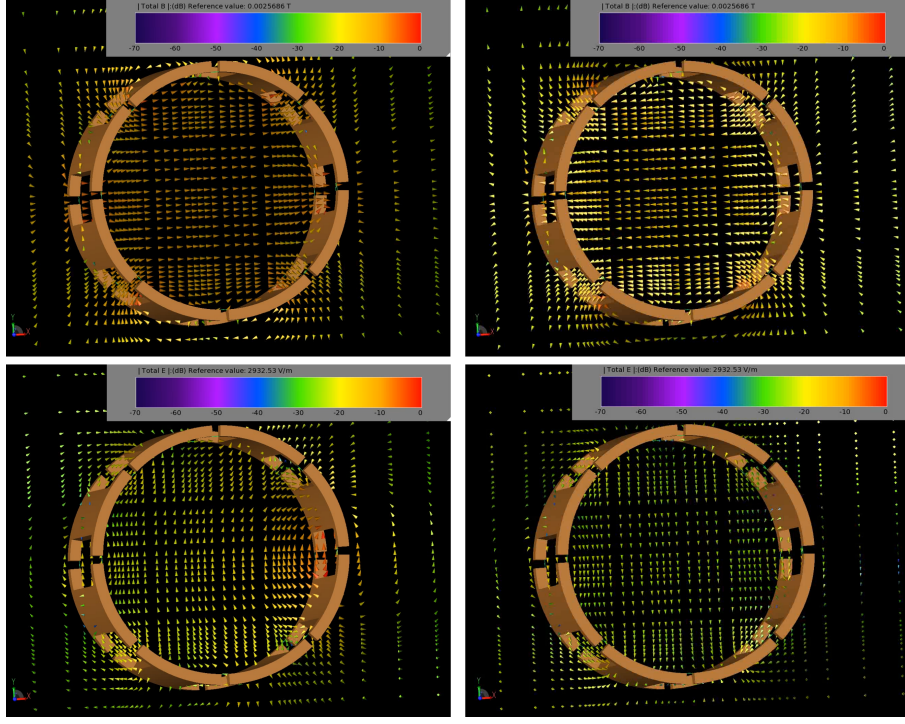


Figure 10: Magnetic Field (above) and Electric Field (below) during in one cycle for a birdcage antenna: linear polarization [6].

impedance change will happen. This requires tuning to shift back to the original resonance condition. This effect has been already seen and solved in MRI machines, as it is caused by the introduction of parts of bodies within the antenna [26], [33]. Tuning can be realized, by moving conducting components that change X_C and X_L next to the antenna. This is implemented in the IPT by the movable injector, and/or by changing position and strength of the DC magnetic field. The assembled IPT is shown in Fig. 11. After resonance verification, ignition is expected by early 2020.

7. Conclusion and Outlook

The IPT based on birdcage antenna has been designed, simulated, and assembled. The birdcage antenna operating at resonance ensure a partially matched load by having $X = 0\Omega$. Moreover, the EM fields configuration produces a drift of ions and electrons towards the same direction providing partial thrust and realizing a neutral plasma plume that does not require a neutralizer. The movable injector can be used for tuning the resonance frequency, as well as the variable DC magnetic field. Verification of the XFDTD simulations against spectrum analyzer is currently ongoing and showing very good agree-

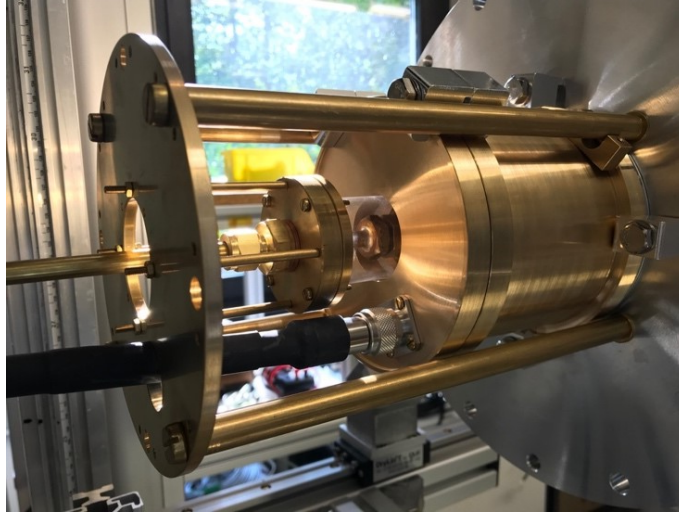


Figure 11: IPT assembled [6].

ment. By early 2020 the IPT will be attempted a first ignition followed by a discharge characterization for different gases, mass flows, powers, and magnetic field strengths. In the next years, the plasma will be evaluated by respective diagnostic tools such as Langmuir and Faraday probes at first, Retarding Potential Analyzer and optical emission spectroscopy as next. Further optimization of the magnetic field configuration is on going to optimize the IPT of thrust generation.

Acknowledgments

This project has received funding from the European Union's Horizon 2020 research and innovation programme under grant agreement No. 737183. This reflects only the author's view and the European Commission is not responsible for any use that may be made of the information it contains.

References

- [1] F. Romano, T. Binder, G. Herdrich, S. Fasoulas, T. Schönherr, Air-intake design investigation for an air-breathing electric propulsion system, 34th International Electric Propulsion Conference, Kobe, Japan (IEPC2015 269b).
- [2] F. Romano, T. Binder, G. Herdrich, T. Schönherr, Intake design for an atmosphere-breathing electric propulsion system, Space Propulsion 2016, Roma, Italy (SP2016 3124981).
- [3] F. Romano, B. Massuti-Ballester, T. Binder, G. Herdrich, S. Fasoulas, T. Schönherr, System analysis and test-bed for an atmosphere-breathing electric propulsion system using an inductive plasma thruster, *Acta Astronautica* 147 (2018) 114 – 126. doi:<https://doi.org/10.1016/j.actaastro.2018.03.031>.
- [4] F. Romano, G. Herdrich, S. Fasoulas, N. C. S. Edmondson, S. Haigh, R. Lyons, V. A. Oiko, P. Roberts, K. Smith, J. Becedas, G. González, I. Vázquez, A. B. nd K. Antonini, K. Bay, L. Ghizoni, V. Jungnell, J. Morsbøl, T. Binder, A. Boxberger, D. Garcia-Almiñana, S. Rodriguez-Donaire, , D. Kataria, M. Davidson, R. Outlaw, B. Belkouchi, A. Conte, J. S. Perez, R. Villain, A. Schwalber, B. Heißerer, Performance evaluation of a novel inductive atmosphere-breathing EP system, 35th International Electric Propulsion Conference, Atlanta, USA (IEPC2017 184).
- [5] F. Romano, G. Herdrich, T. Binder, A. Boxberger, C. Traub, S. Fasoulas, T. Schönherr, P. Roberts, K. Smith, S. Edmondson, S. Haigh, N. Crisp, V. A. Oiko, R. Lyons, S. Worrall, S. Livadiotti, J. Becedas, G. González, R. Domínguez, L. Ghizoni, V. Jungnell, K. Bay, J. Morsbøl, D. Garcia-Almiñana, S. Rodriguez-Donaire, M. Sureda, D. Kataria, R. Outlaw, R. Villain, J. S. Perez, A. Conte, B. Belkouchi, A. Schwalber, B. Heißerer, Effects of applied magnetic field on IPG6-S, test-bed for an ABEP-based inductive plasma thruster (IPT), Space Propulsion 2018, Seville, Spain (SP2018 00412).
- [6] F. Romano, G. Herdrich, P. Roberts, A. Boxberger, Y.-A. Chan, C. Traub, S. Fasoulas, K. Smith, S. Edmondson, S. Haigh, N. Crisp, V. A. Oiko, R. Lyons, S. Worrall, S. Livadiotti, C. Huyton, L. Sinpetru, R. Outlaw, J. Becedas, R. Domínguez, D. González, V. Hanessian, A. Mølgaard, J. Nielsen, M. Bisgaard, D. Garcia-Almiñana, S. Rodriguez-Donaire, M. Sureda, D. Kataria, R. Villain, J. S. Perez, A. Conte, B. Belkouchi, A. Schwalber, B. Heißerer, M. Magarotto, D. Pavarin, Inductive plasma thruster (IPT) for an atmosphere- breathing electric propulsion system: Design and set in operation, 36th International Electric Propulsion Conference, Vienna, Austria (IEPC2019 A488).
- [7] F. Romano, G. Herdrich, P. Roberts, A. Boxberger, Y.-A. Chan, C. Traub, S. Fasoulas, K. Smith, S. Edmondson, S. Haigh, N. Crisp, V. A. Oiko,

- R. Lyons, S. Worrall, S. Livadiotti, C. Huyton, L. Sinpetru, R. Outlaw, J. Becedas, R. Domínguez, D. González, V. Hanessian, A. Mølgaard, J. Nielsen, M. Bisgaard, D. Garcia-Almiñana, S. Rodriguez-Donaire, M. Sureda, D. Kataria, R. Villain, J. S. Perez, A. Conte, B. Belkouchi, A. Schwalber, B. Hei erer, M. Magarotto, D. Pavarin, Inductive plasma thruster (IPT) design for an atmosphere-breathing electric propulsion system (ABEP), 70th International Astronautical Congress, Washington D.C., USA (IAC-19.C4.6.3x49922).
- [8] P. Roberts, N. Crisp, V. Abrao Oiko, S. Edmondson, S. Haigh, C. Huyton, S. Livadiotti, R. Lyons, K. Smith, L. Sinpetru, A. Straker, S. Worrall, F. Romano, G. Herdrich, A. Boxberger, Y.-A. Chan, C. Traub, S. Fasoulas, K. Smith, R. Outlaw, J. Becedas, R. Domínguez, D. González, V. Hanessian, A. Mølgaard, J. Nielsen, M. Bisgaard, D. Garcia-Almiñana, S. Rodriguez-Donaire, M. Sureda, D. Kataria, R. Villain, J. S. Perez, A. Conte, B. Belkouchi, A. Schwalber, B. Hei erer, DISCOVERER – making commercial satellite operations in very low Earth orbit a reality, 70th International Astronautical Congress, Washington D.C., USA (IAC-19.C2.6.1x50774).
- [9] G. Herdrich, M. Fertig, S. L hle, Experimental simulation of high enthalpy planetary entries, *The Open Journal of Plasma Physics* 2, ISSN: 1876-5343 (2009) 150–164 (15). doi:10.2174/1876534300902010150.
- [10] G. Herdrich, D. Petkow, Water-cooled and thin-walled ICP sources: Characterization and MHD-optimization, *Journal of Plasma Physics* 74 (3) (2008) 391–429. doi:10.1017/S0022377807006927.
- [11] A. R. Chadwick, G. Herdrich, M. K. Kim, B. Dally, Transient electromagnetic behaviour in inductive oxygen and argon-oxygen plasmas, *Plasma Sources Science and Technology* 25 (6) (2016) 065025.
- [12] M. Dropmann, G. Herdrich, R. Laufer, D. Puckert, H. Fulge, S. Fasoulas, J. Schmoke, M. Cook, T. W. Hyde, A new inductively driven plasma generator (IPG6) - setup and initial experiments, *IEEE Transactions on Plasma Science* 41 (4) (2013) 804–810.
- [13] S. Masillo, F. Romano, R. Soglia, G. Herdrich, P. Roberts, A. Boxberger, Y.-A. Chan, C. Traub, S. Fasoulas, K. Smith, S. Edmondson, S. Haigh, N. Crisp, V. A. Oiko, R. Lyons, S. Worrall, S. Livadiotti, C. Huyton, L. Sinpetru, R. Outlaw, J. Becedas, R. Domínguez, D. González, V. Hanessian, A. Mølgaard, J. Nielsen, M. Bisgaard, D. Garcia-Almiñana, S. Rodriguez-Donaire, M. Sureda, D. Kataria, R. Villain, J. S. Perez, A. Conte, B. Belkouchi, A. Schwalber, B. Hei erer, M. Magarotto, D. Pavarin., Analysis of electrodeless plasma source enhancement by an externally applied magnetic field for an inductive plasma thruster (IPT), 7th Russian German Conference on Electric Propulsion and Their Application, Rauischholzhausen, Germany (RGCEP2018 A079).

- [14] F. F. Chen, Permanent magnet helicon source for ion propulsion, *IEEE Transactions on Plasma Science* 36 (5) (2008) 2095–2110. doi:10.1109/TPS.2008.2004039.
- [15] G. Cifali, T. Misuri, P. Rossetti, M. Andrenucci, D. Valentian, D. Feili, B. Lotz, Experimental characterization of HET and RIT with atmospheric propellants, in: 32nd International Electric Propulsion Conference, 2011, pp. 11–15.
- [16] G. Cifali, D. Dignani, T. Misuri, P. Rossetti, M. Andrenucci, D. Valentian, F. Marchandise, D. Feili, B. Lotz, Completion of HET and RIT characterization with atmospheric propellants, *Proceedings of Space Propulsion, Bordeaux*.
- [17] T. Andreussi, G. Cifali, V. Giannetti, A. Piragino, E. Ferrato, A. Rossodivita, M. Andrenucci, J. Longo, L. Walpot, Development and experimental validation of a Hall-effect thruster RAM-EP concept, in: 35th International Electric Propulsion Conference, 2017, pp. 8–12.
- [18] T. Andreussi, E. Ferrato, V. Giannetti, A. Piragino, C. A. Paissoni, G. Cifali, M. Andrenucci, Development status and way forward of SITAEL’s air-breathing electric propulsion engine, in: *AIAA Propulsion and Energy 2019 Forum*, 2019, p. 3995.
- [19] F. Romano, G. Herdrich, A. Boxberger, P. Roberts, K. Smith, S. Edmondson, S. Haigh, N. Crisp, V. A. Oiko, R. Lyons, S. Worrall, S. Livadiotti, J. Becedas, G. González, R. Domínguez, L. Ghizoni, V. Jungnell, K. Bay, J. Morsbøl, C. Traub, S. Fasoulas, D. Garcia-Almiñana, S. Rodriguez-Donaire, M. Sureda, D. Kataria, R. Outlaw, R. Villain, J. S. Perez, A. Conte, B. Belkouchi, A. Schwalber, B. Heißerer, Advances on the inductive plasma thruster design for an atmosphere-breathing EP system, 69th International Astronautical Congress, Adelaide, Australia (IAC-18.C4.6.4x46387).
- [20] F. F. Chen, Performance of a permanent-magnet helicon source at 27 and 13 MHz, *Physics of Plasmas* 19 (9) (2012) 093509. doi:10.1063/1.4754580.
- [21] F. Romano, T. Binder, G. Herdrich, P. Roberts, S. Rodriguez-Donaire, D. Garcia-Almiñana, N. Crisp, S. Edmondson, S. Haigh, R. Lyons, V. A. Oiko, K. Smith, J. Becedas, G. González, I. Vázquez, A. B. nd K. Antonini, K. Bay, L. Ghizoni, V. Jungnell, J. Morsbøl, A. Boxberger, S. Fasoulas, D. Kataria, M. Davidson, R. Outlaw, B. Belkouchi, A. Conte, J. S. Perez, R. Villain, A. Schwalber, B. Heißerer, System analysis and test-bed for an atmosphere-breathing electric propulsion system using an inductive plasma thruster, 68th International Astronautical Congress, Adelaide, Australia (IAC-17-C4,6,5,x41810).
- [22] F. F. Chen, D. Arnush, Generalized theory of helicon waves. I. Normal modes, *Physics of Plasmas* 4 (9) (1997) 3411–3421. arXiv:https://doi.

org/10.1063/1.872483, doi:10.1063/1.872483.
URL <https://doi.org/10.1063/1.872483>

- [23] D. Arnush, F. F. Chen, Generalized theory of helicon waves. II. Excitation and absorption, *Physics of Plasmas* 5 (5) (1998) 1239–1254. arXiv:<https://doi.org/10.1063/1.872782>, doi:10.1063/1.872782.
URL <https://doi.org/10.1063/1.872782>
- [24] D. Melazzi, V. Lancellotti, ADAMANT: A surface and volume integral-equation solver for the analysis and design of helicon plasma sources, *Computer Physics Communications* 185 (7) (2014) 1914 – 1925. doi:<https://doi.org/10.1016/j.cpc.2014.03.019>.
- [25] A. W. Kieckhafer, M. L. R. Walker, RF power system for thrust measurements of a helicon plasma source, *Review of Scientific Instruments* 81 (7) (2010) 075106. arXiv:<https://doi.org/10.1063/1.3460263>, doi:10.1063/1.3460263.
URL <https://doi.org/10.1063/1.3460263>
- [26] C. E. Hayes, W. A. Edelstein, J. F. Schenck, O. M. Mueller, M. Eash, An efficient, highly homogeneous radiofrequency coil for whole-body NMR imaging at 1.5 T, *Journal of Magnetic Resonance* (1969) 63 (3) (1985) 622 – 628. doi:[https://doi.org/10.1016/0022-2364\(85\)90257-4](https://doi.org/10.1016/0022-2364(85)90257-4).
- [27] Jian-Ming Jin, *Electromagnetics in magnetic resonance imaging*, *IEEE Antennas and Propagation Magazine* 40 (6) (1998) 7–22. doi:10.1109/74.739187.
- [28] A. Howling, P. Guittienne, C. Hollenstein, I. Furno, Resonant RF network antennas for inductively-coupled plasma sources, in: *Proceeding 41st EPS Conference on Plasma Physics*, Berlin, Germany, 23-27 June 2014, no. CONF, 2014, pp. P2–139.
- [29] I. Furno, R. Agnello, B. Duval, C. Marini, A. Howling, R. Jacquier, P. Guittienne, F. Usel, W. Dirk, S. Alain, B. Stephane, A novel helicon plasma source for negative ion beams for fusion.
URL <http://infoscience.epfl.ch/record/222962>
- [30] I. Furno, R. Agnello, U. Fantz, A. Howling, R. Jacquier, C. Marini, G. Plyushchev, P. Guittienne, A. Simonin, Helicon wave-generated plasmas for negative ion beams for fusion, in: *EPJ Web of Conferences*, Vol. 157, EDP Sciences, 2017, p. 03014.
- [31] P. Guittienne, E. Chevalier, C. Hollenstein, Towards an optimal antenna for helicon waves excitation, *Journal of Applied Physics* 98 (8) (2005) 083304. doi:10.1063/1.2081107.
- [32] R. Jacquier, R. Agnello, B. P. Duteil, P. Guittienne, A. Howling, G. Plyushchev, C. Marini, A. Simonin, I. Morgal, S. Bechu, et al., First

B-dot measurements in the RAID device, an alternative negative ion source for demo neutral beams, Fusion Engineering and Design doi:<https://doi.org/10.1016/j.fusengdes.2019.02.025>.

- [33] A. C. Özen, Novel MRI Technologies for Structural and Functional Imaging of Tissues with Ultra-short T_2 Values, Vol. 34, KIT Scientific Publishing, 2017.